



PERGAMON

Available online at www.sciencedirect.com

SCIENCE @ DIRECT®

Computers
& Structures

Computers and Structures 81 (2003) 1739–1749

www.elsevier.com/locate/comprstruc

A new algorithm for numerical solution of dynamic elastic–plastic hardening and softening problems

Hongwu Zhang^{a,*}, Xinwei Zhang^a, Jiun-Shyan Chen^b

^a *State Key Laboratory of Structural Analysis and Industrial Equipment, Department of Engineering Mechanics, Dalian University of Technology, Dalian 116024, PR China*

^b *Department of Civil and Environment Engineering, University of California, Los Angeles, Los Angeles, CA 90095-1593, USA*

Received 25 September 2002; accepted 4 March 2003

Abstract

The objective of this paper is to develop a new algorithm for numerical solution of dynamic elastic–plastic strain hardening/softening problems, particularly for the implementation of the gradient dependent model used in solving strain softening problems. The new algorithm for the solution of dynamic elastic–plastic problems is derived based on the parametric variational principle. The gradient dependent model is employed in the numerical model to overcome the mesh-sensitivity difficulty in dynamic strain softening or strain localization analysis. The precise integration method, which has been used for the solution of linear problems, is adopted and improved for the solution of dynamic non-linear equations. The new algorithm is proposed by taking the advantages of the parametric quadratic programming method and the precise integration method. Results of numerical examples demonstrate the validity and the advantages of the proposed algorithm.

© 2003 Elsevier Science Ltd. All rights reserved.

Keywords: Elasto-plasticity; Precise integration method; Parametric quadratic programming method; Gradient dependent model; Dynamic response

1. Introduction

Traditionally, incremental iteration method is widely used in non-linear problems. However, it often faces the problem of low convergent speed, especially for the super-non-linear problems such as post-buckling and strain softening problems. Based on the parametric variational principle [23,26], the parametric quadratic programming method was developed as an effective way to solve the non-linear problems. By introducing mathematical programming method, the parametric quadratic programming method avoids the iteration procedures. For elastic–plastic problem, this method avoids the limitation of the Drucker hypothesis. It can also be applied to the non-associated plastic constitutive

model, non-normal sliding and strain softening problems [20,23].

In the past several decades, many kinds of time integration methods (see [1,2]) have been proposed. Recently, Zhong [25] proposed a precise integration method, which has many advantages such as absolute stability, zero-amplitude rate of decay, zero-period specific elongation and non-overstep properties. This method has been used successfully in many linear dynamic problems [9,12] and heat conduction [21] problems. The discussion of the method was recently given by Zhang and Zhong [22] where the optimum parameters selection was suggested. In this paper, the parametric variational principle is generalized for the dynamic analysis of the elastic–plastic strain hardening/softening problems. The parametric quadratic programming method combined with the precise integration method is adopted to solve the dynamic elastic–plastic hardening/softening problems.

* Corresponding author. Tel./fax: +86-411-4708769.
E-mail address: zhanghw@dlut.edu.cn (H. Zhang).

A large number of engineering materials can be classified as softening materials in which localized large strain are observed. This is called the strain softening or localization problem [11,17]. This phenomenon often acts as a precursor of structural failure and has a determinant effect on the deformation of the structure. Numerical simulation of such kind of non-linear problems is generally more difficult than that of the linear dynamic problems [3]. It has been proved mathematically that the mesh sensitivity problem exists when the finite element method is carried out in the analysis of the softening materials [13,16]. The dependence on the discretization is not only with respect to mesh refinement but also with respect to mesh alignment. If the classical constitutive model is adopted directly in these softening materials, the initial value problem becomes ill-posed and cannot describe the underlying physics properly.

So far, the following three methods are the most effective in overcoming the above mesh sensitivity problem: rate-dependent model ([10,15,19], etc.), Cosserat constitutive model ([14], etc.), non-local and gradient model [3,6,7]. A reproducing kernel regularization method [26] has been proposed as a generalization of non-local and gradient models without the need of additional boundary conditions. In this paper, the gradient model is used to overcome the mesh sensitivity problem. As the Laplacian of the hardening/softening parameter is embedded in the material constitutive equations, we obtain not the algebra equations but the differential equations from the constitutive equations. This remarkably increases the complexity in the numerical implementation [6] of the algorithm. de Borst and Muhlhaus [6] solved the problem successfully by introduction of unknown quantities (displacement and plastic multiplier) in each node. One important work in this paper is to develop a new algorithm for the implementation of the gradient dependent model in the finite element analysis.

Section 2 of this paper describes the gradient dependent model and the corresponding formulation. Section 3 presents the parametric variational principle and the parametric quadratic programming method for the gradient dependent model in the dynamic analysis. In Section 4, the Newmark integration method is adopted in the discretization of time domain. In Section 5, the precise integration method is introduced in the numerical solution of the dynamic elastic–plastic hardening/softening equations. Finally, numerical examples are given to verify the theory and algorithm proposed in this paper.

2. Formulation of the gradient dependent model

In the conventional plasticity theory, the yield function \mathbf{f} depends on the parameters of stress $\boldsymbol{\sigma}$, plastic

strain $\boldsymbol{\varepsilon}^p$ and some internal variables. Without loss of generalities, the isotropic hardening/softening materials is considered here, and the yield function can be defined as

$$\mathbf{f} = \mathbf{f}(\boldsymbol{\sigma}, \boldsymbol{\varepsilon}^p, \boldsymbol{\kappa}) \quad (1)$$

In gradient dependent model, the yield function can be written as

$$\mathbf{f} = \mathbf{f}(\boldsymbol{\sigma}, \boldsymbol{\varepsilon}^p, \boldsymbol{\kappa}, \nabla^2 \boldsymbol{\kappa}) \quad (2)$$

where $\boldsymbol{\kappa}$ is the hardening/softening parameter in the constitutive model.

It can be seen that the main difference between the conventional plasticity theory and the gradient dependent plasticity model is the introducing of the gradient of softening/hardening parameters in the yield function. Therefore, in gradient dependent plasticity, the yield status of a material point is not only related to its own plastic parameters but also under the influence of the plastic parameters in the neighboring region. The size of the influence region is determined by the internal length scale in the gradient dependent model. According to the gradient dependent model, the plastic deformation in a point will expand to a certain region.

Based on the gradient dependent model, the elastic–plastic constitutive equations can be defined as follows

$$d\boldsymbol{\sigma} = \mathbf{D}(d\boldsymbol{\varepsilon} - d\boldsymbol{\varepsilon}^p), \quad d\boldsymbol{\varepsilon}^p = \left(\frac{\partial \mathbf{g}}{\partial \boldsymbol{\sigma}} \right) \boldsymbol{\lambda} \quad (3)$$

$$\mathbf{f}(\boldsymbol{\sigma}, \boldsymbol{\varepsilon}^p, \boldsymbol{\kappa}, \nabla^2 \boldsymbol{\kappa}) \leq 0, \quad \boldsymbol{\lambda} = \begin{cases} \geq 0 & \text{when } \mathbf{f} = 0 \\ = 0 & \text{when } \mathbf{f} < 0 \end{cases} \quad (4)$$

where $\boldsymbol{\lambda}$ is the plastic flow multiplier; \mathbf{g} is the plastic potential surface. The Von-Mises yield function \mathbf{f} is adopted in the numerical examples which will be shown in Section 6.

Without loss of generality, we assume $d\boldsymbol{\kappa} = h\boldsymbol{\lambda}$, $\bar{c} = h(\partial \mathbf{f} / (\partial \nabla^2 \boldsymbol{\kappa}))$, and h is the hardening/softening modulus.

Applying Taylor expansion to Eq. (4), we obtain the consistent equation

$$\mathbf{f}_0 + \mathbf{W}d\boldsymbol{\varepsilon} - \mathbf{M}\boldsymbol{\lambda} + \bar{c}\nabla^2 \boldsymbol{\lambda} \leq 0, \quad \boldsymbol{\lambda} \geq 0 \quad (5)$$

where

$$\mathbf{W} = \left(\frac{\partial \mathbf{f}}{\partial \boldsymbol{\sigma}} \right)^T \mathbf{D},$$

$$\mathbf{M} = \mathbf{W} \left(\frac{\partial \mathbf{g}}{\partial \boldsymbol{\sigma}} \right) - \left(\frac{\partial \mathbf{f}}{\partial \boldsymbol{\varepsilon}^p} \right)^T \left(\frac{\partial \mathbf{g}}{\partial \boldsymbol{\sigma}} \right)^T + \frac{\partial \mathbf{f}}{\partial \boldsymbol{\kappa}} h \quad (6)$$

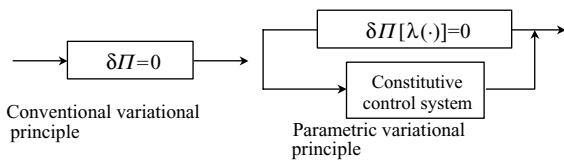
in which \bar{c} is the parameter of the gradient dependent model or the internal length scale parameter.

3. Parametric variational principle for elastic–plastic problems with the gradient dependent model

3.1. Parametric variational principle

The parametric variational principle is the application of optimum system control theory to the unspecified boundary value problems in continuum mechanics. In this principle, the constitutive relations of the physical phenomena are taken into account by means of the selection of some proper state and control variables such as those used in a control system. Thus the parametric variational method can be used for solution of the problems where the conventional variational principles are not being successful, and it also simplifies the solution process.

The parametric variational principle contains two kinds of state variables in its variational function. The first kind are variables such as the displacements of the structure which will take part in the variation process, whereas the other one, such as the plastic multipliers is taken as a control variable during the variational process, and is determined by the minimization/maximization of the variational function. On the other hand, the material constitutive relations work just as a control system in the boundary value problems during the whole variational process. The differences between the parametric variational principle and the conventional variational principle can be shown by the following figure:



The parametric minimum potential energy principle based on the gradient dependent model for the dynamic non-linear problems can be described as follows: for all of the possible incremental displacement solutions which satisfy the strain–displacement relations and displacement boundary conditions, the exact solution minimizes the potential energy of the system

$$\Pi = \int_{t_1}^{t_2} \left\{ \int_{\Omega} \left[\frac{1}{2} \dot{d}u_i \rho \dot{d}u_i - \frac{1}{2} du_{i,j} D_{ijkl} du_{k,l} + \lambda_i R_{kli} du_{k,l} + db_i du_i \right] d\Omega - \int_{\Gamma_p} \bar{d}p_i du_i d\Gamma \right\} dt \quad (7)$$

at the control of the system state equations

$$f_0 + Wd\epsilon - M\lambda + \bar{c}\nabla^2\lambda + v = 0, \quad \lambda^T v = 0, \quad \lambda, v \geq 0 \quad (8)$$

Here, b_i is the body force, $R_{klm} = (\partial g_m / \partial \sigma_{ij}) D_{ijkl}$, and v is the slack vector. This problem can be stated as

$$\min. \quad \Pi[\lambda(\cdot)] \quad (9)$$

$$\text{s.t.} \quad f(\mathbf{du}, \lambda, \nabla^2\lambda) + v = 0, \quad \lambda^T v = 0, \quad \lambda, v \geq 0 \quad (10)$$

where λ is the parametric variable which does not take part in the variation process but controls the system state varying between elastic and plastic ones. \mathbf{du} is the incremental displacement vector, and \mathbf{dp} is the load vector. Eq. (10) is the system control equation derived from the constitutive relations.

3.2. Parametric quadratic programming method

To solve the non-linear problem, the general algorithm is to take the linearization of the non-linear equations in conjunction with the incremental iteration. In contrast, the parametric quadratic programming method adopts the algorithm of the programming theory in the algebra solution without iteration processes. A detail description and summary of the discretization procedure can be found in the work by Zhang et al. [24]. The discretized finite element equations of the non-linear dynamic problem can be expressed as

$$\begin{cases} M\ddot{u} + Kdu - \lambda\Phi = dP \\ Cdu - U\lambda - d + v = 0 \\ \lambda^T v = 0, \quad \lambda, v \geq 0 \end{cases} \quad (11)$$

where

$$\begin{aligned} M &= \int_{\Omega} \rho N^T N d\Omega, \quad K = \int_{\Omega} B^T DB d\Omega, \\ dP &= \int_{\Gamma_p} N^T d\bar{p} d\Gamma \end{aligned} \quad (12)$$

are the mass matrix, stiffness matrix and load vector, respectively. These matrices and vector have the same meaning as those of the conventional finite element method. The new matrices and vectors generated by the parametric variational principle are

$$\Phi = \int_{\Omega} N_{L,j}^u D_{ijkl}^e \frac{\partial g_{\beta}}{\partial \sigma_{ij}} d\Omega, \quad C = \int_{\Omega} W_{kl\beta} N_{m,l}^u d\Omega \quad (13)$$

$$U = \int_{\Omega} (MN_m^{\lambda} + \bar{c}\nabla^2 N^{\lambda}) d\Omega, \quad d = - \int_{\Omega} f_0 d\Omega \quad (14)$$

where Φ is the plastic potential matrix which represents the plastic potential of the system, C is the constrained matrix which represents the constraint status, and U is the hardening matrix which indicates the hardening status. For the associated flow rule, the plastic potential matrix is the transposition of the constrained matrix, i.e. $\Phi = C^T$. d and v are the constraint and slack vectors, and λ is the parametric vector whose physical meaning is the plastic flow parameter.

It can be seen clearly that the introduction of the gradient dependent model only adds the gradient item

into the hardening matrix. In the parametric quadratic programming algorithm, quadratic interpolation for the parametric λ is needed.

If the damping effect is considered, the damping matrix needs to be added in the dynamic equation, we have

$$\mathbf{M}\ddot{\mathbf{u}} + \mathbf{G}\dot{\mathbf{u}} + \mathbf{K}\mathbf{u} - \lambda\Phi = \mathbf{dP} \tag{15}$$

where \mathbf{G} is the damping matrix.

The incremental displacement can be solved with the discretization of the dynamic equation in time domain. Substituting the incremental displacement into the control equation results in a quadratic programming problem which can be solved by many methods such as the Wolf method and Lemke method [4,8].

4. Discretization in time domain with the Newmark time integration algorithm

Discretization in time domain of dynamic equation (15) is carried out by means of the Newmark scheme at first. The algorithm can be expressed as

$$\begin{cases} \dot{\mathbf{u}}_{t+\Delta t} = \dot{\mathbf{u}}_t + [(1-\gamma)\ddot{\mathbf{u}}_t + \gamma\ddot{\mathbf{u}}_{t+\Delta t}]\Delta t \\ \mathbf{u}_{t+\Delta t} = \mathbf{u}_t + \dot{\mathbf{u}}_t\Delta t + [(0.5-\beta)\ddot{\mathbf{u}}_t + \beta\ddot{\mathbf{u}}_{t+\Delta t}]\Delta t^2 \end{cases} \tag{16}$$

where γ, β are the integration parameters of the Newmark scheme.

From Eq. (16) the incremental formulations of the Newmark scheme can be obtained by the following expressions

$$\begin{cases} \mathbf{d}\dot{\mathbf{u}} = [(1-\gamma)\ddot{\mathbf{u}}_t + \gamma\ddot{\mathbf{u}}_{t+\Delta t}]\Delta t \\ \mathbf{d}\mathbf{u} = \dot{\mathbf{u}}_t\Delta t + [(0.5-\beta)\ddot{\mathbf{u}}_t + \beta\ddot{\mathbf{u}}_{t+\Delta t}]\Delta t^2 \end{cases} \tag{17}$$

Then the incremental velocity and acceleration are of the following formulations

$$\begin{cases} \Delta\ddot{\mathbf{u}} = \frac{1}{\beta\Delta t^2}[\Delta\mathbf{u} - \dot{\mathbf{u}}_t\Delta t - 0.5\Delta t^2\ddot{\mathbf{u}}_t] \\ \Delta\dot{\mathbf{u}} = \ddot{\mathbf{u}}_t\Delta t + \frac{\gamma}{\beta\Delta t}[\Delta\mathbf{u} - \Delta t\dot{\mathbf{u}}_t - 0.5\Delta t^2\ddot{\mathbf{u}}_t] \end{cases} \tag{18}$$

Substituting Eq. (18) into (11), we obtain

$$\overline{\mathbf{K}}\Delta\mathbf{u} - \lambda\Phi = \overline{\mathbf{F}} \tag{19}$$

where

$$\begin{cases} \overline{\mathbf{K}} = \mathbf{K} + \frac{1}{\beta\Delta t^2}\mathbf{M} + \frac{\gamma}{\beta\Delta t}\mathbf{G} \\ \overline{\mathbf{F}} = \Delta\mathbf{F} + \mathbf{M}\left[\frac{1}{\beta\Delta t}\dot{\mathbf{u}}_t + \frac{1}{2\beta}\ddot{\mathbf{u}}_t\right] + \mathbf{G}\left[\frac{\gamma}{\beta}\dot{\mathbf{u}}_t + \left(\frac{\gamma}{2\beta} - 1\right)\Delta t\ddot{\mathbf{u}}_t\right] \end{cases} \tag{20}$$

are the effective stiffness matrix and effective load vector respectively.

The dynamic elastic–plastic problem is now changed into the following quadratic programming problem

$$\begin{cases} \overline{\mathbf{K}}\mathbf{d}\mathbf{u} - \lambda\Phi = \overline{\mathbf{F}} \\ \mathbf{C}\mathbf{d}\mathbf{u} - \mathbf{U}\lambda - \mathbf{d} + \mathbf{v} = \mathbf{0} \\ \lambda^T\mathbf{v} = 0, \quad \lambda, \mathbf{v} \geq 0 \end{cases} \tag{21}$$

which is a generalized formulation of a linear complementary problem.

Remark 1. What difference between the algorithm developed here and the conventional iteration method is that the iteration progress in the new algorithm is performed by the solution of the parametric programming problem (21). For instance, in the well known Lemke’s algorithm, the base/pivot exchange is generally needed so that the complementary conditions can be satisfied. The physical meaning of this base/pivot exchange is just like the re-calculation of the element stress state after the residual force is computed. This is the reason why the important iteration procedure and consistent tangent matrix (see [2,18]) are not calculated explicitly in the method proposed here.

5. Precise integration method in time domain

5.1. General scheme of the precise integration method for solution of dynamic elastic–plastic problems

The precise integration method is a new algorithm for numerical solution of differential equations. It has the absolute stability, zero-amplitude rate of decay, zero-period specific elongation and non-overstep properties. We extend this method here to the numerical solution of dynamic elastic–plastic problems.

Considering the dynamic equation

$$\mathbf{M}\ddot{\mathbf{u}} + \mathbf{K}\mathbf{u} - \lambda\Phi = \mathbf{F} \tag{22}$$

and combining with the identical equation $\{\dot{\mathbf{u}}\} = \{\dot{\mathbf{u}}\}$, we obtain the following differential equation

$$\dot{\mathbf{V}} = \mathbf{H}\mathbf{V} + \mathbf{r} + \Phi^*\lambda^* \tag{23}$$

where

$$\begin{aligned} \mathbf{V} &= \begin{Bmatrix} \mathbf{u} \\ \dot{\mathbf{u}} \end{Bmatrix}; \quad \mathbf{H} = \begin{bmatrix} \mathbf{0} & \mathbf{I} \\ -\mathbf{M}^{-1}\mathbf{K} & \mathbf{0} \end{bmatrix}; \quad \mathbf{r} = \begin{Bmatrix} \mathbf{0} \\ \mathbf{M}^{-1}\mathbf{F}(t) \end{Bmatrix}; \\ \Phi^* &= \begin{Bmatrix} \mathbf{0} & \mathbf{0} \\ \mathbf{M}^{-1}\Phi & \mathbf{0} \end{Bmatrix}; \quad \lambda^* = \begin{Bmatrix} \lambda \\ \mathbf{0} \end{Bmatrix} \end{aligned} \tag{24}$$

The homogeneous solution of Eq. (23) is

$$\mathbf{V}(t) = [\mathbf{T}(\tau)]\mathbf{C} \tag{25}$$

where

$$[\mathbf{T}(\tau)] = \exp([\mathbf{H}] \times \tau) \tag{26}$$

In the integrative step $t \in [t_k, t_{k+1}]$, $\tau = t - t_k$, \mathbf{C} is a constant vector and decided by the initial conditions of the incremental step.

The key step in Eq. (26) is the evaluation of the exponential matrix \mathbf{T} . Precise integration method provides a scheme (2^N algorithm) to compute the exponential matrix precisely. At first, the evaluation of the exponential matrix of (26) is evaluated as

$$\mathbf{T} = e^{\mathbf{A}} = (e^{\mathbf{A}'})^m \tag{27}$$

where

$$\mathbf{A}' = \mathbf{A}/m, \quad \mathbf{A} = \mathbf{H}\tau, \quad m = 2^N$$

N is a numerical parameter, and a constant value $N = 20$ was proposed in Zhong [25]. Then $e^{\mathbf{A}'}$ is evaluated by the power series ($p \geq 1$)

$$e^{\mathbf{A}'} \cong \sum_{i=0}^p \frac{\mathbf{A}'^i}{i!} = \mathbf{I} + \mathbf{T}_a, \quad \mathbf{T}_a = \sum_{i=1}^p \frac{\mathbf{A}'^i}{i!} \tag{28}$$

From Eqs. (27) and (28), the computation matrix \mathbf{T} can be furthermore expressed as

$$\begin{aligned} \mathbf{T} = e^{\mathbf{A}} &= (\mathbf{I} + \mathbf{T}_a)^{2^N} = (\mathbf{I} + \mathbf{T}_a)^{2^{N-1}} (\mathbf{I} + \mathbf{T}_a)^{2^{N-1}} \\ &= (\mathbf{I} + 2\mathbf{T}_a + \mathbf{T}_a^2)^{2^{N-1}} \end{aligned} \tag{29}$$

Note that in the precise integration method the unit matrix \mathbf{I} should not be directly included in the computation of (29), as to reduce the round off error. The following procedures are recommended

Step I:

$$\mathbf{T}_a \Leftarrow 2\mathbf{T}_a + \mathbf{T}_a^2 \tag{30}$$

and after N times loop, the exponential matrix will be obtained by

Step II:

$$\mathbf{T} = e^{\mathbf{A}} = \mathbf{I} + \mathbf{T}_a \tag{31}$$

The particular solution of the Eq. (23) is

$$\begin{aligned} \mathbf{V}_p(t) &= -\mathbf{H}^{-1}[\mathbf{r}_0 + \mathbf{H}^{-1}\mathbf{r}_1 + \mathbf{r}_1(t - t_k)] \\ &\quad - \mathbf{H}^{-1}[\Phi^* \lambda_0^* + \mathbf{H}^{-1}\Phi^* \lambda_1^* + \Phi^* \lambda_1^*(t - t_k)] \end{aligned} \tag{32}$$

The general solution of Eq. (23) is

$$\mathbf{V}(t) = [\mathbf{T}(\tau)](\mathbf{V}(t_k) - \mathbf{V}_p(t_k)) + \mathbf{V}_p(t) \tag{33}$$

where \mathbf{r}_0 , \mathbf{r}_1 , λ_0 and λ_1 are constants.

Substituting Eq. (32) into (33) and letting $\Delta\lambda^* = \lambda_1^*(t - t_k)$, $\tau = t - t_k$, the general solution is obtained

$$\begin{aligned} \mathbf{V}(t_{k+1}) &= \left[\mathbf{T}_a \mathbf{H}^{-1} \mathbf{H}^{-1} \Phi^* \Delta\lambda^* \frac{1}{\tau} - \mathbf{H}^{-1} \Phi^* \Delta\lambda^* \right] \\ &\quad + \mathbf{T}_a \mathbf{H}^{-1} \Phi^* \lambda_0^* + \bar{\mathbf{V}}(t_{k+1}) \end{aligned} \tag{34}$$

where

$$\begin{aligned} \bar{\mathbf{V}}(t_{k+1}) &= \mathbf{T}[\mathbf{V}(t_k) + \mathbf{H}^{-1}(\mathbf{r}_0 + \mathbf{H}^{-1}\mathbf{r}_1)] \\ &\quad - \mathbf{H}^{-1}[\mathbf{r}_0 + \mathbf{H}^{-1}\mathbf{r}_1 + \mathbf{r}_1\tau] \end{aligned} \tag{35}$$

$$\mathbf{T}_a = \mathbf{T} - \mathbf{I} \tag{36}$$

when the structure is linear elastic, the parametric variable λ is zero. Then the above integrative scheme (34) will reduce to $\bar{\mathbf{V}}_{k+1}$ which is the linear solution shown in Zhong [25] and Zhang and Zhong [22].

5.2. Solution technique of the method proposed

From Eq. (34), the incremental solution of the problem (23) is

$$\begin{aligned} \Delta\mathbf{V}(t_{k+1}) &= \mathbf{V}(t_{k+1}) - \mathbf{V}(t_k) \\ &= \left[\mathbf{T}_a \mathbf{H}^{-1} \mathbf{H}^{-1} \Phi^* \Delta\lambda^* \frac{1}{\tau} - \mathbf{H}^{-1} \Phi^* \Delta\lambda^* \right] \\ &\quad + \mathbf{T}_a \mathbf{H}^{-1} \Phi^* \lambda_0^* + \bar{\mathbf{V}}(t_{k+1}) - \mathbf{V}(t_k) \end{aligned} \tag{37}$$

In the precise integration method, the dimension of the status vector \mathbf{V}_{k+1} is doubled so that the dynamic equation can be reduced into first order differential equation. It is therefore that the dimension of the system control equation needs also to be doubled

$$\mathbf{C}^* \Delta\mathbf{V}(t_{k+1}) - \mathbf{U}^* \Delta\lambda^* - \mathbf{d}^* + \mathbf{v}^* = 0 \tag{38}$$

where

$$\begin{aligned} \mathbf{C}^* &= \begin{bmatrix} \mathbf{C} & \mathbf{0} \\ \mathbf{0} & \mathbf{0} \end{bmatrix}, \quad \mathbf{U}^* = \begin{bmatrix} \mathbf{U} & \mathbf{0} \\ \mathbf{0} & \mathbf{0} \end{bmatrix}, \quad \mathbf{d}^* = \begin{bmatrix} \mathbf{d} \\ \mathbf{0} \end{bmatrix}, \\ \Delta\lambda^* &= \begin{bmatrix} \Delta\lambda \\ \mathbf{0} \end{bmatrix}, \quad \mathbf{v}^* = \begin{bmatrix} \mathbf{v} \\ \mathbf{0} \end{bmatrix} \end{aligned} \tag{39}$$

Substituting the incremental general solution (37) into the system control equation (38), we have

$$\begin{aligned} \mathbf{v}^* + \mathbf{C}^* \left[\mathbf{T}_a \mathbf{H}^{-1} \mathbf{H}^{-1} \Phi^* \frac{1}{\tau} - \mathbf{H}^{-1} \Phi^* \right] \Delta\lambda^* - \mathbf{U}^* \Delta\lambda^* \\ = \mathbf{d} - \mathbf{C}^* [\bar{\mathbf{V}}_{k+1} - \mathbf{V}_k] - \mathbf{C}^* \mathbf{T}_a \mathbf{H}^{-1} \Phi^* \lambda_0^* \end{aligned} \tag{40}$$

where

$$\begin{aligned} \mathbf{C}^* \left[\mathbf{T}_a \mathbf{H}^{-1} \mathbf{H}^{-1} \Phi^* \frac{1}{\tau} - \mathbf{H}^{-1} \Phi^* \right] \\ = \begin{bmatrix} -\mathbf{C} \left(\frac{\mathbf{T}_{a12}}{\tau} - \mathbf{I} \right) \mathbf{K}^{-1} \Phi \\ \mathbf{0} \end{bmatrix} \end{aligned} \tag{41a}$$

$$\bar{\mathbf{V}}(t_{k+1}) - \mathbf{V}(t_k) = \begin{bmatrix} \bar{\mathbf{u}}(t_{k+1}) - \mathbf{u}(t_k) \\ \bar{\dot{\mathbf{u}}}(t_{k+1}) - \dot{\mathbf{u}}(t_k) \end{bmatrix} \tag{41b}$$

$$\mathbf{C}^* \mathbf{T}_a \mathbf{H}^{-1} \Phi^* \lambda_0^* = \begin{bmatrix} -\mathbf{C} \mathbf{T}_{a11} \mathbf{K}^{-1} \Phi \lambda_0 \\ \mathbf{0} \end{bmatrix} \tag{41c}$$

For the numerical implementation, the above equation can be rewritten as the following form

$$\begin{aligned} & \begin{Bmatrix} \mathbf{v} \\ \mathbf{0} \end{Bmatrix} + \begin{bmatrix} -\mathbf{C}(\frac{\mathbf{T}_{a12}}{\tau} - \mathbf{I})\mathbf{K}^{-1}\Phi\Delta\lambda \\ \mathbf{0} \end{bmatrix} - \begin{Bmatrix} \mathbf{U}\Delta\lambda \\ \mathbf{0} \end{Bmatrix} \\ &= \begin{Bmatrix} \mathbf{d} \\ \mathbf{0} \end{Bmatrix} - \begin{bmatrix} \mathbf{C} & \mathbf{0} \\ \mathbf{0} & \mathbf{0} \end{bmatrix} \begin{Bmatrix} (\bar{\mathbf{u}}_{k+1} - \mathbf{u}_k) \\ (\bar{\dot{\mathbf{u}}}_{k+1} - \dot{\mathbf{u}}_k) \end{Bmatrix} \\ & \quad - \begin{bmatrix} -\mathbf{C}\mathbf{T}_{a11}\mathbf{K}^{-1}\Phi\lambda_0 \\ \mathbf{0} \end{bmatrix} \end{aligned} \tag{42}$$

5.3. Implementation of the algorithm

The implementation of the algorithm proposed can be concluded briefly as what follows:

- (1) Forming the matrices \mathbf{H} , \mathbf{H}^{-1} and \mathbf{T} , the load vectors \mathbf{r}_0 and \mathbf{r}_1 , generating the sub-matrices \mathbf{T}_{a11} , \mathbf{T}_{a12} and \mathbf{T}_{a22} of the matrix \mathbf{T} .
- (2) Time integration for each time step.
 - (1) Forming element and global plastic potential matrix Φ , constraint matrix \mathbf{C} , hardening matrix \mathbf{U} and constraint vector \mathbf{d} .
 - (2) Calculating $\bar{\mathbf{V}}(t_{k+1})$, which corresponds to the elastic solution.
 - (3) Calculating $\Delta\mathbf{V}_{k+1}$ from Eq. (41b) and generating the incremental displacement vector $\bar{\mathbf{u}}(t_{k+1}) - \mathbf{u}(t_k)$.
 - (4) Calculating the coefficient matrices in Eq. (42), substituting the incremental displacement vector $\bar{\mathbf{u}}(t_{k+1}) - \mathbf{u}(t_k)$ into Eq. (42), and taking computation of items at the right side.
 - (5) Solving quadratic programming problem (42) and obtaining the incremental parametric variable $\Delta\lambda$.
 - (6) Substituting the incremental parametric variable $\Delta\lambda$ into Eq. (34), obtaining the status variable and displacement vectors of the current step.
 - (7) If the total integration steps have not been finished, then returning to step (1) and going on the computation of the next time step. Otherwise, the computation is completed.
- (3) Stop.

Remark 2. It is worthwhile to take an analysis and comparison about the time cost and operation number of matrix products used respectively in the precise and Newmark integration algorithms. It should be noticed that the matrices \mathbf{H} , \mathbf{T} and \mathbf{K} used in the precise integration method are constant during the integration process step by step. So some matrices in Eq. (42) can be calculated at the first time integration step and can be used directly in the steps after that. Comparing with the operation number used in the Newmark method, the key part in the precise integration method is in the computation of (41b) where the incremental displacement and velocity are performed. So the operation in Eq. (35) is rather important for the computation cost of the algo-

rihm. For a very general load case, i.e. that the \mathbf{r}_0 and \mathbf{r}_1 are time dependent, the operation number of matrix product will be increased by a factor of 4. In this way, the computation cost will be greater than that used by the Newmark method. However, for some special load cases, such as when \mathbf{r}_0 and \mathbf{r}_1 are constant, the operation number will be the same as that of the Newmark method. On the other hand, due to the high accuracy of the precise integration method, generally, the time step size can be greater than that permitted for Newmark method. Thus, we can conclude that the precise integration method is more effective particularly when the high accuracy results are needed in the numerical simulations. The disadvantages of the method are that for a general case of the problem, the time cost can be larger than that needed when the Newmark method is used.

Remark 3. It will be also noticed from above description that the computation cost for the programming method developed here are almost the same for the solution of the plastic models with or without gradient dependent item. This is due to the fact that only the matrix \mathbf{U} in Eq. (14) is modified when the gradient dependent model is adopted. This additional calculation is only performed on the element level when the element matrix \mathbf{U} is generated.

6. Numerical examples

Example 6.1 (One truss structure is showed in Fig. 1). The length of top, bottom and vertical trusses is 1 m. The cross sections of all trusses are $1.0 \times 10^{-3} \text{ m}^2$. The material parameters are $E = 210 \text{ GPa}$; $\rho = 7800 \text{ kg/m}^3$. The load applied on the truss joint is $2.0 \times 10^3 \text{ N}$ as shown in Fig. 1. We consider here the simple hardening material strain–stress relation as plotted in Fig. 2. The yield stress is $4.0 \times 10^6 \text{ Pa}$. Because the first order of free vibration period of the structure is 0.01335 s, the length of time step are respectively selected as 3.0×10^{-4} , 1.5×10^{-4} and $0.75 \times 10^{-4} \text{ s}$. The corresponding numbers of the time step are 30, 60 and 120. With the precise integration method, the displacement of Y direction of the point where the load is applied is calculated in the situations of the elasticity and plasticity respectively. The displacement results are showed in Figs. 3–5 where the value of total time is the same but divided into dif-

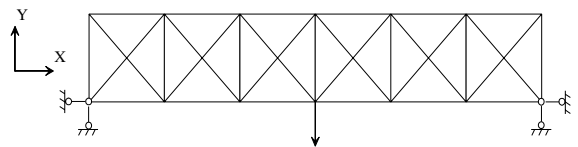


Fig. 1. Two-dimensional truss model.

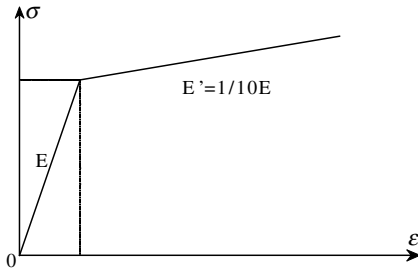


Fig. 2. Strain–stress relationships for two-dimensional truss and elastic–plastic cantilever plate.

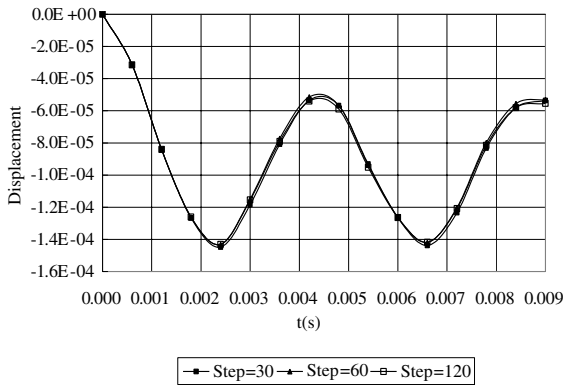


Fig. 3. Results obtained by the precise integration method with different lengths of time step (total time = 0.009 s).

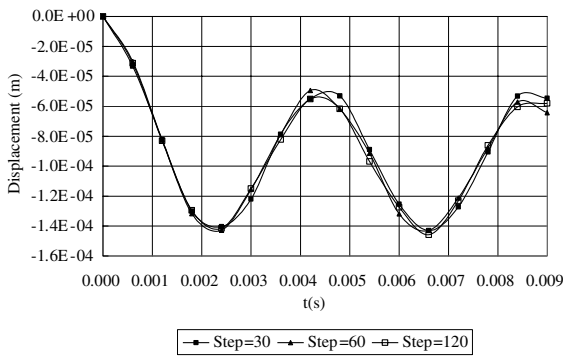


Fig. 4. Results obtained by the Newmark method with different lengths of time step (total time = 0.009 s).

ferent time steps. It can be seen that the results of the precise integration method are less dependent on the length of time step than that of the Newmark method. As it is showed in Fig. 5, the results of the Newmark method with 180 steps is rather closed to that obtained by the precise integration method with 30 time steps. This means the precise integration method has more

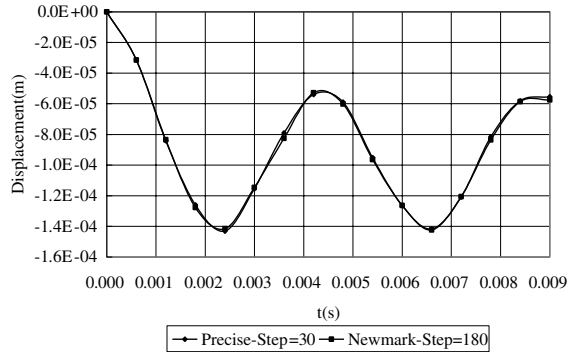


Fig. 5. Comparison between the results obtained by the precise integration method with 30 time steps and the Newmark method with 180 time steps.

advantage on the computation accuracy. For the computation efficacy, the precise integration method with 120 time steps has the same computational time as the Newmark method with 180 steps. If we use the precise integration method with 30 steps, the computational accuracy is closed to the Newmark method with 180 steps and the computational time is reduced remarkably.

Example 6.2 (*Dynamic response of an elastic–plastic cantilever plate*). It is shown in Fig. 6 that a cantilever plate works with a jump load on the top surface. The curve of strain–stress relationship is the same as shown in Fig. 2. Von-Mises constitutive model is adopted. The material parameters are: Young’s modulus $E = 20.5$ GPa, mass density $\rho = 7.8 \times 10^3$ kg/m³, Poisson ratio $\nu = 0.3$, plastic yield stress is 20 GPa, plate thickness is 5 mm. 30, 60 and 120 time steps are calculated and the lengths of time step are respectively selected as 4.0×10^{-3} , 2.0×10^{-3} and 1.0×10^{-3} s. The displacement with time variation in vertical direction of point A is shown respectively in Figs. 7–9. Fig. 7 shows the comparison among the results obtained by the precise integration method with different lengths of integration time step. Fig. 8 further gives the corresponding results obtained by the Newmark integration method. Fig. 9 shows the comparison between the results obtained respectively by the precise integration method with large time step and the Newmark one with small time step.

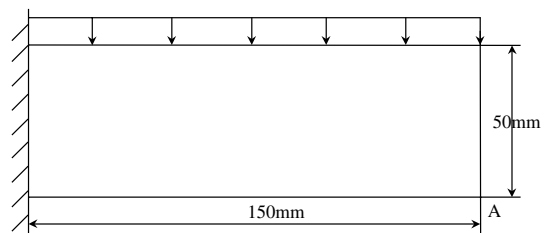


Fig. 6. An elastic–plastic cantilever plate.

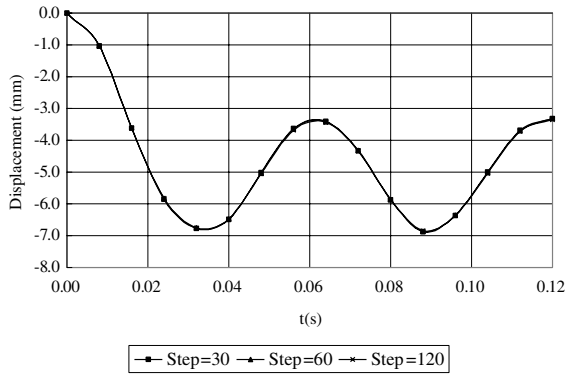


Fig. 7. Comparison among results obtained by the precise integration method with different lengths of time step.

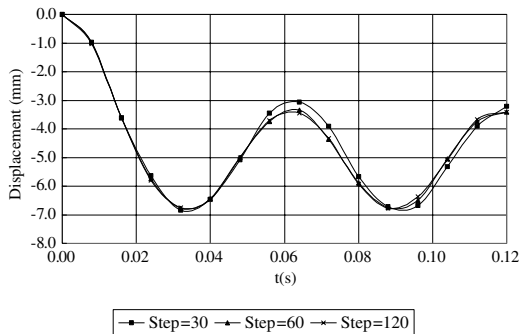


Fig. 8. Comparison among results obtained by the Newmark integration method with different lengths of time step.

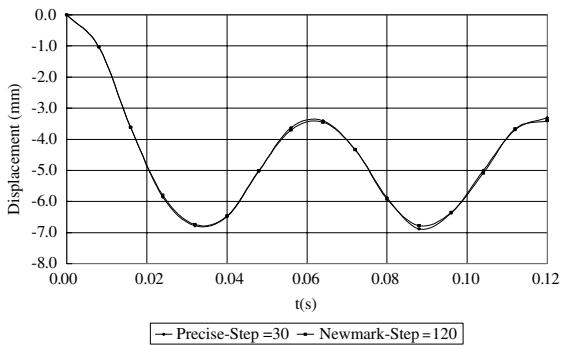


Fig. 9. Comparison between results obtained by the precise and Newmark integration methods with large and small lengths of time step.

Obviously, it can be observed that the results with the precise integration method are not so sensitivity to the length of time step as those obtained by the Newmark algorithm. With a large length of time step, the precise integration method can obtain high accuracy results as those obtain by Newmark integration method with a

small length of time step. This is the same as that obtained in the previous example.

Example 6.3 (One-dimensional bar in the tension and strain softening state). The strain softening problem is sketched in Figs. 10–12. Load: $q_0 = 0.75$ N; material: $E = 20$ GPa, $\rho = 2000.0$ kg/m³, $h = -2.0$ GPa. The yield stress in Von-Mises plasticity model is 2.0 MPa; $\bar{c} = 5 \times 10^4$ N.

The mesh sensitivity problem can be checked easily by the results obtained by this example. The bar is divided into 10, 20 and 40 elements respectively. In Fig. 13 the strain results at $t = 4.2 \times 10^{-5}$ s with the different meshes are plotted after the dynamic wave reflects from the left boundary. Mesh sensitivity results are obvious: strain localization and the width of the localization zone decreases when more elements are used.

The problem is now computed with the gradient dependent model. The bar is divided into 20, 40, 80 and 160 elements respectively. Parameters $h = -2.0$ GPa, $\bar{c} = 5 \times 10^4$ N and the length of time step = 1.5×10^{-7} s. The strain localization along the bar at $t = 1.8 \times 10^{-5}$ s is given in Fig. 14. It can be seen that the width of the plastic zone keeps constant with the different mesh.

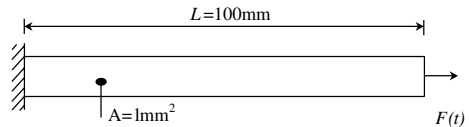


Fig. 10. One-dimensional bar in the tension and softening state.

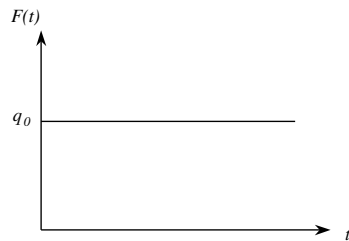


Fig. 11. Load-time relationship for one-dimensional bar.

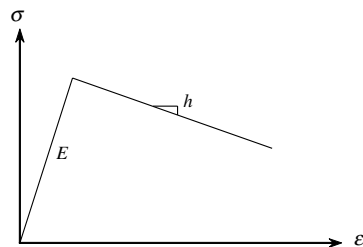


Fig. 12. Stress-strain relationship for one-dimensional bar.

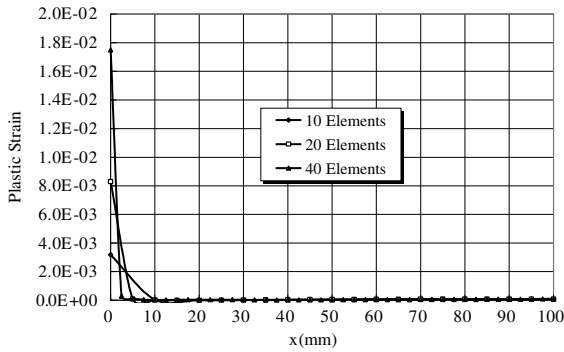


Fig. 13. Mesh sensitivity problem in one-dimensional case.

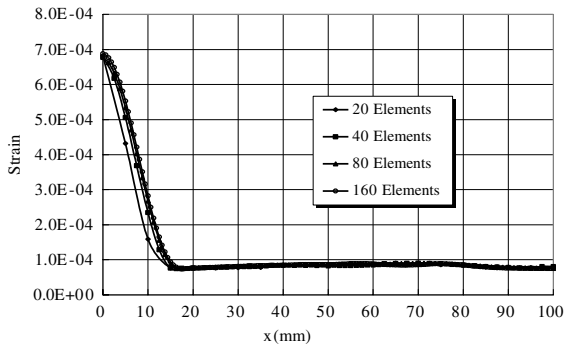


Fig. 14. Strain localization along the bar obtained by the different meshes with the gradient dependent model.

From $l = \sqrt{-\bar{c}/h}$, the material internal length scale parameter $l = 5$ mm. The corresponding width of the localization zone is 15.7 mm which is just the half value of $2\pi l$. The similar results have been also announced in the work by de Borst and Muhlhaus [6].

In Fig. 15, the strain localization results along the bar with the different internal length scale parameters are given. The values of \bar{c} are 1.25×10^4 , 2.5×10^4 , 5.0×10^4 , 10.0×10^4 , 20.0×10^4 N respectively, and the corresponding internal length scale values obtained are

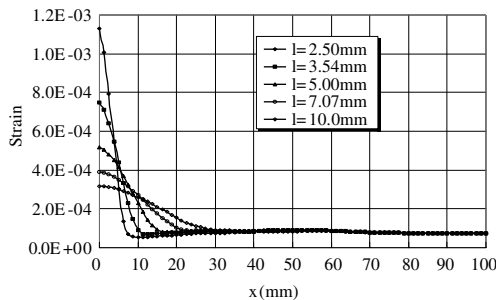


Fig. 15. Numerical results with different internal length scale parameters.

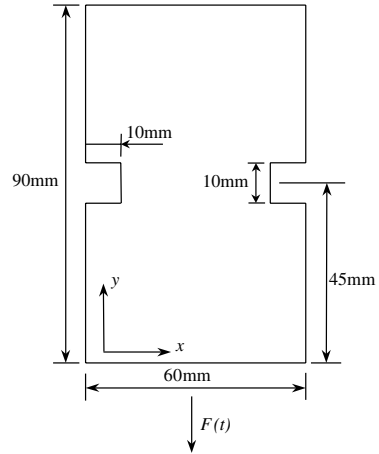


Fig. 16. Impact test of a double-notched specimen.

shown in Fig. 16 from 2.50 to 10.0 mm. The numerical results are rather closed to the theory solutions with the different internal length scale parameters.

Example 6.4 (Impact test of a double-notched specimen). The geometry of the problem is shown in Fig. 16. The load–time relation is plotted in Fig. 17. Von-Mises plasticity model is used and the material parameters are: $q_0 = 3.5 \times 10^6$ N/m, $t_0 = 3.5 \times 10^{-5}$ s; $E = 40.7$ GPa, $\rho = 2350.0$ kg/m³, $h = -2.5$ GPa. The yield stress of the material is 4.0 GPa; $\bar{c} = 5 \times 10^4$ N. Two kinds of finite element meshes are adopted in the computation.

In Fig. 18a and b, the results of structural deformation at time 5.0×10^{-5} s with different meshes based on the conventional constitutive relation are given. It can be seen clearly that the differences between the results of these two meshes, especially in the notched area where the material changes into softening. The structural deformation results at time 5.0×10^{-5} s with different meshes based on the gradient dependent model are given in Fig. 19a and b. The results of the coarse mesh is closed to the fine mesh's, especially in the notched area. This embodies again the advantages of the gradient dependent model.

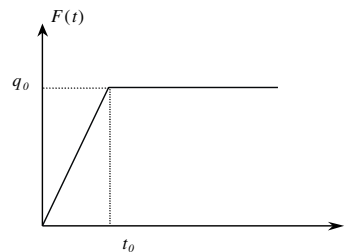


Fig. 17. Load–time relationship for impact test of a double-notched specimen.

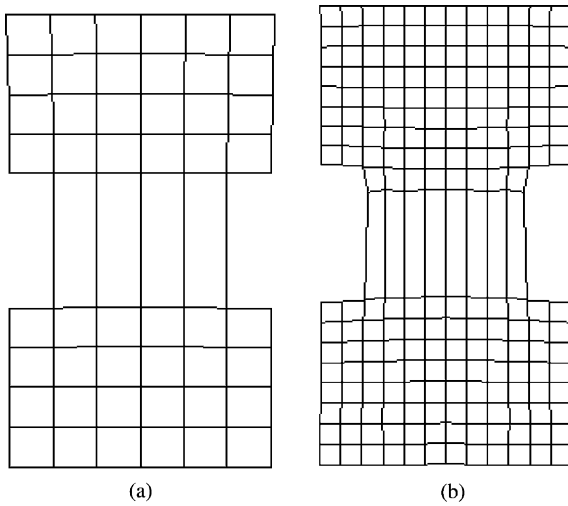


Fig. 18. Results of structural deformation with the conventional constitutive model. (a) Coarse mesh and (b) fine mesh.

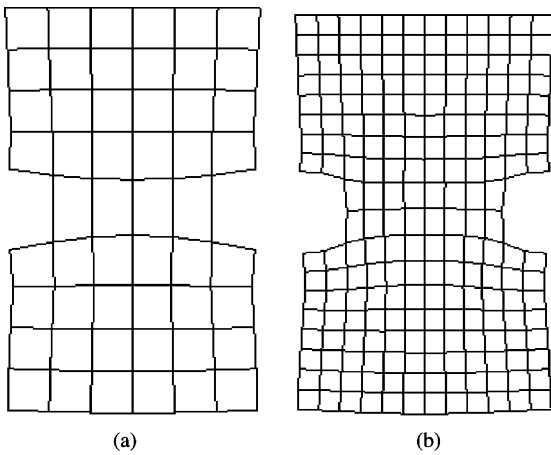


Fig. 19. Results of structural deformation based on the gradient dependent model. (a) Coarse mesh and (b) fine mesh.

In Figs. 20 and 21, the axial strains in the center section of the specimen are given with the different meshes based on the conventional constitutive model and the gradient dependent model. The mesh dependence existing in the conventional constitutive model is observed. On the contrary, the results of the gradient dependent model possesses well property which embodies the expanding of the localization area.

Remark 4. It has been pointed that in elastoplastic dynamics with softening, the contractivity of perturbation (algorithmic stability) is crucial. Algorithms unconditionally stable for non-softening constitutive models become “conditionally stable” (or even unconditionally unstable) in the presence of softening [5]. However, this

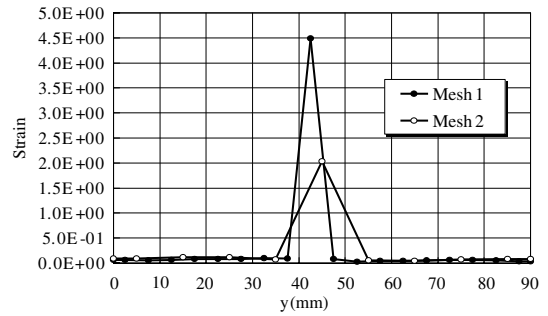


Fig. 20. Axial strain in the center section of the specimen based on the conventional constitutive model. Mesh 1: fine mesh, Mesh 2: coarse mesh.

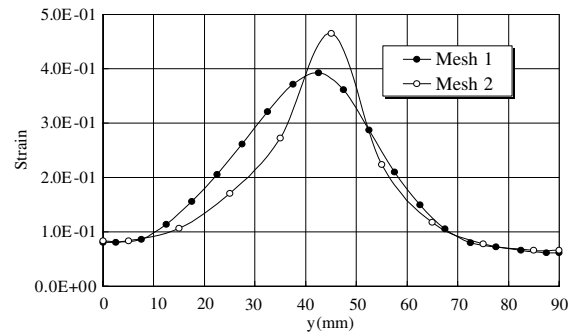


Fig. 21. Axial strain in the center section of the specimen based on the gradient dependent model. Mesh 1: fine mesh, Mesh 2: coarse mesh.

phenomenon does not occur in the computation of the numerical examples with softening described above, and the algorithm presents still unconditional stable such as that used for non-softening constitutive models. This shows on the other hand the advantages of the algorithm developed in this paper.

7. Conclusions

What presented above described a new algorithm for numerical simulation of elastic–plastic strain hardening/softening problems. The gradient dependent model based on the non-local theory was adopted to overcome the mesh dependent problem in the analysis of the dynamic strain softening problem. For the numerical analysis, the parametric variational principle is adopted which makes the gradient dependent model be easily implemented in the algorithm. Furthermore, a parametric quadratic programming algorithm combined with both the Newmark and the precise integration methods in time domain is derived and changes the problem into a linear complementary problem. Numer-

ical examples are given and the results demonstrate the validity and efficiency of the theory and algorithm presented in this paper.

Acknowledgements

The financial supports from the National Key Basic Research Special Foundation (G1999032805), the Scientific Fund for National Outstanding Youth of China, the National Natural Science Foundation of China (10225212, 50178016, 19872016) and the Foundation for University Key Teacher by the Ministry of Education of China are greatly acknowledged.

References

- [1] Bathe KJ. Numerical methods in finite element analysis. New Jersey: Prentice-Hall; 1976.
- [2] Bathe KJ. Finite element procedures. New Jersey: Prentice-Hall; 1996.
- [3] Bazant ZP, Cabot PG. Nonlocal continuum damage, localization instability and convergence. ASME, J Appl Mech 1988;55:287–93.
- [4] Bazaraa MS, Shetty CM. Nonlinear programming, theory and algorithms. New York: John Wiley & Sons; 1979. p. 1979.
- [5] Comi C, Corigliano A, Maier G. Dynamic analysis of elastoplastic softening discretized structures. J Eng Mech, ASCE 1992;118(12):2352–75.
- [6] de Borst R, Mühlhaus HB. Gradient-dependent plasticity: formulation and algorithmic aspects. Int J Numer Meth Eng 1992;35:521–39.
- [7] de Borst R, Pamin J. Gradient plasticity in numerical simulation of concrete cracking. Eur J Mech, A/Solids 1996;15:295–320.
- [8] Ferris MC et al. Applications and algorithms of complementarity. Kluwer Acad Publ; 2001.
- [9] Fung TC. A precise time step integration method by step-response and impulsive-response matrices for dynamic problems. Int J Numer Meth Eng 1997;40:4501–27.
- [10] Fusao O, Toshihisa A, Atsushi Y. A strain localization analysis using a viscoplastic softening model for clay. Int J Plast 1995;11:523–45.
- [11] Hill R. Acceleration waves in solids. J Mech Phys Solids 1962;10:1–16.
- [12] Kong XD. Precise time integration algorithms of ordinary differential equations and application in multibody system dynamics. PhD Dissertation, Dalian University of Technology, Dalian, China, 1998.
- [13] Lasry D, Belytschko TB. Localization limiters in transient problems. Int J Solids Struct 1988;24:581–97.
- [14] Mühlhaus HB, Vardoulakis I. The thickness of shear band in granular materials. Geotechnique 1987;37:271–83.
- [15] Needleman A. Material rate dependence and mesh sensitivity in localization problems. Comp Meth Appl Eng 1988;67:69–85.
- [16] Read HE, Hegemier GA. Strain softening of rock, soil and concrete—a review article. Mech Mater 1984;3:271–94.
- [17] Rice JR. On the stability of dilatant hardening for saturated rock masses. J Geophys Res 1975;80:1531–6.
- [18] Simo JC, Hughes TJR. Computational inelasticity. New York: Springer-Verlag Inc.; 1998.
- [19] Sluys LJ. Wave propagation, localization and dispersion in softening solids. PhD thesis, Civil Engineering Department of Delft University of Technology, 1992.
- [20] Zhang HW, Schrefler BA. Gradient-dependent plasticity model and dynamic strain localization analysis of saturated and partially saturated porous media: one dimensional model. Eur J Solid Mech A/Solids 2000; 19(3):503–24.
- [21] Zhang HW, Zhang P, Zhong WX. A precise integration method for the quasi-analytical solution of heat conduction. Mech Pract 1998a;20(4):9–11.
- [22] Zhang HW, Zhong WX. Discussions about numerical computation of the matrix exponential. J Dalian Univ Technol 2000;40(5):522–5.
- [23] Chen JS, Wu CT, Belytschko T. Regularization of material instabilities by meshfree approximations with intrinsic length scales. Int J Numer Meth Eng 2000;47:1301–22.
- [24] Zhang HW, Zhong WX, Gu YX. A combined parametric quadratic programming and iteration method for 3D elastic–plastic frictional contact problem analysis. Comput Meth Appl Mech 1998b;155:307–24.
- [25] Zhong WX. Precise integration method for structural dynamic analysis. J Dalian Univ Technol 1994;34(2): 131–6.
- [26] Zhong WX, Zhang HW, Wu CW. Parametric variational principle and its applications in engineering. Beijing: Science Press; 1997.